Phenylboronic Acid-Installed Polymeric Micelles for Targeting Sialylated Epitopes in Solid Tumors

Stephanie Deshayes,[†,◆] Horacio Cabral,[‡,◆] Takehiko Ishii,[‡] Yutaka Miura,[§,∥] Shutaro Kobayashi,[†] Takashi Yamashita,[⊥] Akira Matsumoto,[#] Yuji Miyahara,[#] Nobuhiro Nishiyama,[○] and Kazunori Kataoka*[†,‡,∥,∇]

[†]Department of Materials Engineering, [‡]Department of Bioengineering, [§]Division of Tissue Engineering, and [∥]Center for Disease Biology and Integrative Medicine, Graduate School of Engineering, The University of Tokyo, 7-3-1 Hongo, Bunkyo-ku, Tokyo 113-8656, Japan

[⊥]Department of Pure and Applied Chemistry, Graduate School of Science and Technology, Tokyo University of Science, 2641 Yamazaki, Noda-shi, Chiba-ken 278-8510, Japan

[#]Institute of Biomaterials and Bioengineering, Tokyo Medical and Dental University, 2-3-10 Kanda-Surugadai, TokyoChiyoda-ku, 101-0062, Japan

[○]Polymer Chemistry Division, Chemical Resources Laboratory, Tokyo Institute of Technology, R1-11, 4259 Nagatsuta, Midori-ku, Yokohama 226-8503, Japan

[∇]Center for NanoBio Integration, The University of Tokyo, 7-3-1 Hongo, Bunkyo-ku, Tokyo 113-8656, Japan

S *Supporting Information*

ABSTRACT: Ligand-mediated targeting of nanocarriers to tumors is an attractive strategy for increasing the efficiency of chemotherapies. Sialylated glycans represent a propitious target as they are broadly overexpressed in tumor cells. Because phenylboronic acid (PBA) can selectively recognize sialic acid (SA), herein, we developed PBA-installed micellar nanocarriers incorporating the parent complex of the anticancer drug oxaliplatin, for targeting sialylated epitopes overexpressed on cancer cells. Following PBA-installation, the micelles showed high affinity for SA, as confirmed by fluorescence spectroscopy even at intratumoral pH conditions, i.e., pH 6.5, improving their cellular recognition and uptake and enhancing their *in vitro* cytotoxicity against B16F10 murine melanoma cells. *In vivo*, PBA-installed micelles effectively reduced the growth rate of both orthotopic and lung metastasis models of melanoma, suggesting the potential of PBA-installed nanocarriers for enhanced tumor targeting
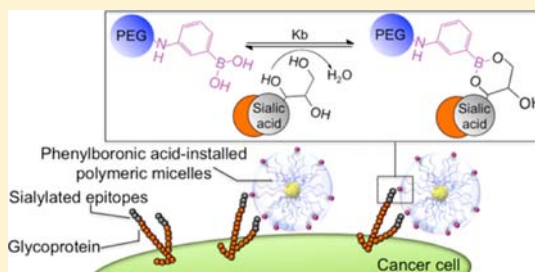
INTRODUCTION

Nanocarriers have shown great potential for selectively delivering high payloads of therapeutic molecules to tumors.[1−5] When systemically injected, long-circulating nanocarriers can specifically accumulate in solid tumors due to the increased permeability of the tumor vasculature and be retained because of the impaired lymphatic drainage at the cancerous site.[6] By functionalization of the surface of these nanocarriers with ligands capable of recognition of cell-specific surface receptors, they can be rendered with cellular selectivity and superior intracellular delivery.[2,3,7−12] Thus, antibodies,[8] antibody fragments,[9] aptamers,[10] peptides,[11,12] and small molecules[13] have been used as ligands for improving the tumor targeting ability of nanocarriers. The efficiency of ligand-installed nanocarriers for targeting cancer cells is affected by several features, such as the binding affinity of the ligands to the receptors, the rate of internalization, the density and availability of the receptors, the intratumoral distribution of the receptors and the variation of the receptor expression with the tumor stage.[7−13] Therefore, effective approaches for ligand-mediated targeting of nano-

carriers require suitable recognition of the versatile receptor landscapes of tumors.

Carbohydrate antigens, which are expressed in all tumor cells due to aberrant glycosylation[14−16] represent an exceptional target for ligand-mediated targeting of nanocarriers, as they are displayed in tumors more frequently than oncogene markers, such as HER2/neu.[15] These malignant glycophenotypes overexpress sialylated epitopes, i.e., glycan chains containing *N*-acetylneuraminic acid (Neu5Ac), which is the predominant sialic acid (SA) in humans.[14−16] The increased expression of sialylated antigens on cancer cells is closely related with cancer progression and with poor prognosis in patients with lung, breast, colon, prostate, bladder, and stomach cancer.[14−16] Moreover, hypoxic regions of solid tumors have shown increased levels of sialylated antigens,[17] and the overexpression of sialylated glycans, such as Sialyl-Lewis[x] and Sialyl-Lewis[a], is important for the formation of metastases.[18] SA has been
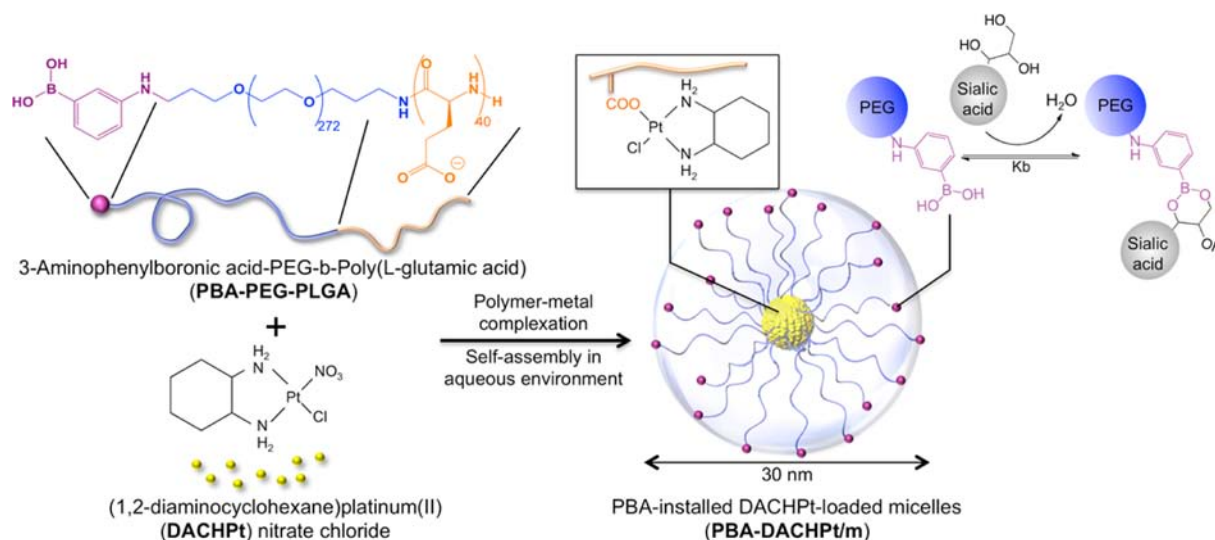
Figure 1. Preparation of PBA-installed DACHPt-loaded micelles by self-assembly through polymer−metal complex formation between DACHPt and PBA-poly(ethylene glycol)-*b*-poly(L-glutamic acid) in distilled water. PBA moieties on the surface of the micelles can bind to SA.

targeted *in vitro* by using lectin[19] and antibodies,[20] such as the tumoral marker CA19-9, used for detection of Sialyl-Lewis[a] in gastrointestinal tumors. Nevertheless, these approaches have been difficult to translate *in vivo*, mainly because of their immunogenicity. Moreover, as SA is also present on red blood cells and the luminal surfaces of vascular endothelium,[21,22] systemically injected ligands for SA targeting should not be active until reaching the site of tumors.

We have recently demonstrated the ability of phenylboronic acid (PBA) for selective recognition of SA overexpressed on the surface of cancer cells.[23] Although PBA can also form complexes with other common sugars, they are unstable unless formed at pHs higher than its pK_a value, whereas the complex between PBA and SA is stable even at pHs lower than its pK_a.[24,25] This feature, with controlled pK_a of PBA, provides a molecular basis for the specific SA recognition at physiological pH. This interaction has been recently used for determining the sialylation status of solid tumors by MRI through PBA-based reporters.[26] In addition to the high affinity and selectivity for SA, PBA presents several advantages for targeting of cancer cells such as being nontoxic, nonimmunogenic, and inexpensive.

Herein, we developed PBA-functionalized nanocarriers by installing PBA moieties on the polymeric micelles for specific targeting of SA epitopes overexpressed on tumor cells. Polymeric micelles, i.e., core−shell self-assemblies of block copolymers, provide multiple advantages as nanocarriers including their nanoscaled size, their poly(ethylene glycol) (PEG) shell, which prevents their recognition by macrophages of the reticuloendothelial system (RES) and prolongs their blood circulation time, and hydrophobic core for loading and controlled release of bioactive molecules.[4,5,27−29] Our polymeric micelles incorporating the anticancer drugs paclitaxel, SN-38, cisplatin, and the parent complex of oxaliplatin, i.e., dichloro(1,2-diamino-cyclohexane)platinum(II) (DACHPt), have advanced to clinical studies,[30,31] demonstrating high efficacy against several intractable tumors, such as triple-negative breast cancers, and less side effects in patients.[30] In this study, we use DACHPt-loaded micelles (DACHPt/m), which have shown selective accumulation in tumor tissues and strong suppression of the growth of several tumor models,[32−35] to

prepare polymeric micelles having PBA moieties on their surface. The micelles were self-assembled through the coordination bond between platinum drug and the carboxylic groups of PBA-poly(ethylene glycol)-*b*-poly(L-glutamic acid) [PBA-PEG-*b*-PLGA] copolymers in water (Figure 1). The inherent fluorescence of PBA installed to PEG-*b*-PLGA copolymers was used for studying its binding affinity against different sugars by fluorescence spectroscopy. Moreover, the ability of PBA-installed DACHPt/m (PBA-DACHPt/m) to target SA in tumors was evaluated *in vitro* as well as *in vivo* against orthotopic and metastatic tumor models. For this purpose, highly metastatic B16F10 murine melanoma cells overexpressing SA on their surface[36] were used, for which we have recently established a method of quantification based on the PBA-SA interaction.[23] Our results showed a high selectivity of PBA-DACHPt/m to SA epitopes, which enhanced their cellular uptake *in vitro* and improved their tumor accumulation and retention *in vivo*, leading to a superior antitumor effect.
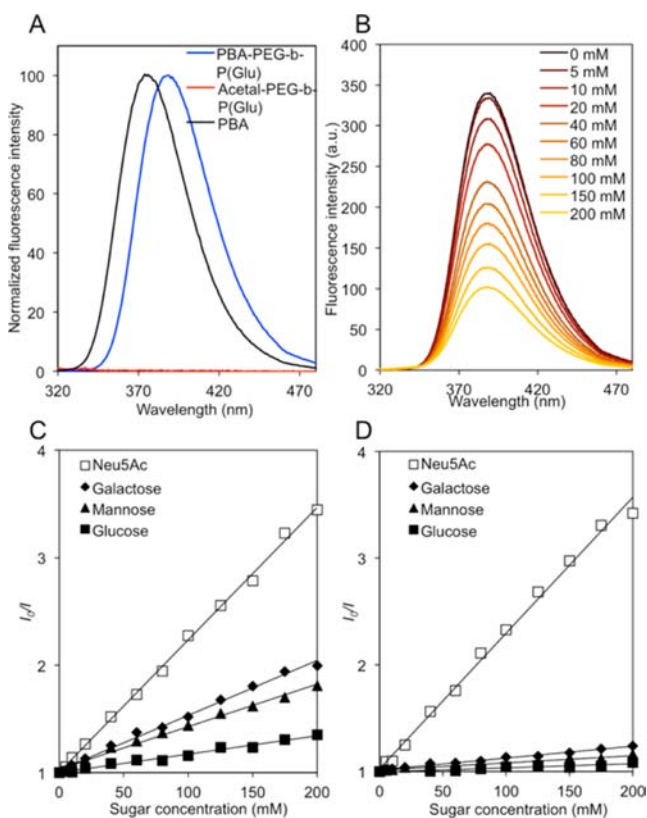
■ RESULTS AND DISCUSSION

Preparation of PBA End-Functionalized PEG-*b*-PLGA. Acetal-poly(ethylene glycol)-*b*-poly(L-glutamic acid) [acetal-PEG-*b*-PLGA] block copolymer was reacted with 3-aminophenylboronic acid by one pot reductive amination to afford aminophenylboronic acid-poly(ethylene glycol)-*b*-poly(L-glutamic acid) [PBA-PEG-*b*-PLGA] copolymer (Scheme S1). Thus, after deprotection of the acetal residue under acidic conditions, the obtained aldehyde group formed a Schiff base with 3-amino-substituted PBA. This intermediate imine was reduced to a secondary amine by using NaBH3CN. The PBA installation at PEG end was confirmed to be almost quantitative by the proton ratios of the aromatic group of PBA and the ethylene units in PEG in the ^{1}H NMR spectrum (Figure S1).

Binding Affinities of PBA-PEG-*b*-PLGA to Various Sugars. Most sugars can complex only with the tetrahedral anionic form of boronate, because the complex with the trigonal neutral form is usually susceptible to hydrolysis.[37] In contrast, SA-PBA complexation is also favored by the trigonal form, for which involvement of multiple metastable binding sites along with intramolecular stabilization via B−N or B−O interactions are likely to play roles.[24,38,39] The pK_a value of the

polymer conjugated PBA, as assessed by fluorescence titration (Figure S2), was determined to be 9.7. This value, which is safely higher than that of physiological conditions, indicates predominant fraction of trigonal (undissociated) PBA at pH 7.4 and, thus, warrants specificity to SA.

To demonstrate the specificity of the PBA modified polymer for SA, we evaluated the binding affinities of PBA-PEG-*b*-PLGA for a series of sugars, such as glucose, mannose, galactose, Neu5Ac, and 2-O-methyl-*α*-D-*N*-acetylneuraminic acid (Me-Neu5Ac; Me-SA), which is a model for neuraminic residues present in the terminal positions of glycan chains,[40] by steady-state fluorescence quenching measurements. While the complexation of sugars has been reported to alter the fluorescence of boron-containing fluorophores,[41,42] in this study, we took advantage of the intrinsic fluorescence property of PBA-PEG-*b*-PLGA. The fluorescence property of PBA was maintained after PBA conjugation to the polymer end (Figure 2A). Moreover, because the binding of PBA to sugars is affected by pH,[37] we perform the experiments at pH 7.4, i.e., physiological pH, and at pH 6.5, which is the lowest environmental pH found inside tumors.[43] The fluorescence spectra of PBA-PEG-*b*-PLGA were collected in the presence of glucose, galactose, mannose, or Neu5Ac. Figure 2B shows the

representative fluorescence spectra of PBA-PEG-*b*-PLGA on addition of Neu5Ac at pH 7.4, illustrating a quenching of fluorescence to occur due to photoinduced electron transfer (PET) as a result of the PBA-Neu5Ac complexation.[44,45] Accordingly, the relative fluorescence intensities of PBA-PEG-*b*-PLGA as a function of sugar concentration at pH 7.4 are shown in Figure 2C and at pH 6.5 in Figure 2D. The kinetic of the fluorescence quenching follows the Stern−Volmer equation (eq 1):

$$I_0/I = 1 + K_b \cdot [Q] = 1 + k_q'' \cdot \tau_0 \cdot [Q] \qquad (1)$$

where I_0 represents the initial fluorescence intensity of the PBA-PEG-*b*-PLGA without sugar, I is the fluorescence intensity of the PBA-PEG-*b*-PLGA in the presence of the sugar (quencher), K_b is the binding constant (M^{-1}), k_q is the quencher rate coefficient ($M^{-1}s^{-1}$), τ_0 is the fluorescence lifetime of PBA-PEG-*b*-PLGA without quencher, and $[Q]$ is the concentration of the quencher.

The binding constants are given as a slope in the Stern−Volmer plot (Figure 2C,D) and reported in Table 1.

**Table 1. Binding Constants and Rate Coefficients of PBA-PEG-*b*-PLGA and Sugars in Phosphate Buffer pH 7.4 and 6.5[a]**

sugar		pH		K_b 6.5/ K_b 7.4
		7.4	6.5	
glucose	K_b (M^{-1})	1.71	0.39	0.29
	$k_q \times 10^{-9}$ ($M^{-1} \cdot s^{-1}$)	0.18	0.04	−
mannose	K_b (M^{-1})	3.95	0.70	0.17
	$k_q \times 10^{-9}$ ($M^{-1} \cdot s^{-1}$)	0.41	0.07	−
galactose	K_b (M^{-1})	5.11	1.11	0.21
	$k_q \times 10^{-9}$ ($M^{-1} \cdot s^{-1}$)	0.53	0.11	−
Neu5Ac (SA)	K_b (M^{-1})	12.3	12.7	1.03
	$k_q \times 10^{-9}$ ($M^{-1} \cdot s^{-1}$)	1.28	1.32	−
MeNeu5Ac (Me-SA)	K_b (M^{-1})	3.40	6.00	1.76
	$k_q \times 10^{-9}$ ($M^{-1} \cdot s^{-1}$)	0.35	0.62	−

[a]Determined by steady-state fluorescence quenching measurements; τ_0 (ns) at pH 7.4 was 9.62 ± 49.2 and at pH 6.5 was 9.67 ± 49.2.

Figure 2. (A) Emission spectra of PBA, Acetal-PEG-*b*-PLGA and PBA-PEG-*b*-PLGA in phosphate buffer (0.1 M, pH 7.4) at room temperature, λ_{ex} = 302 nm. B. Emission spectra of PBA-PEG-*b*-PLGA (40 μM) in phosphate buffer solution (0.1 M, pH 7.4) containing various concentrations of Neu5Ac (0−200 mM) at room temperature, λ_{ex} = 302 nm. Relative fluorescence as a function of sugar concentration for PBA-PEG-*b*-PLGA measured in phosphate buffer (0.1 M) at room temperature (λ_{ex} = 302 nm and λ_{em} = 388 nm) at pH 7.4 (C) and pH 6.5 (D). I_0 and I represent the fluorescence intensity in the absence and presence of sugar respectively. Data were fit according to Stern−Volmer equation (eq 1).

Furthermore, the quencher rate coefficients were assessed from the fluorescence lifetimes (Table 1), which remained unchanged for these pHs (6.5 and 7.4). We observed that the binding constants and the quencher rate coefficients were remarkably higher for Neu5Ac than those for other sugars, indicating a stronger affinity for SA. The binding constant values showed similar tendency with previously reported values using other boronic acids and different methods (UV,[46] ^{11}B-NMR,[24] or indirect fluorescence through the fluorescent reporter compound, Alizarin Red S[47]). Moreover, even though the affinity for sugars depends on the nature of boronic acid, a trend for the selectivity was noticed as SA ≫ galactose ≥ mannose ≅ glucose. It is worth noticing that the ratio between the binding constant at intratumoral pH, i.e., K_b 6.5, and that for pH 7.4, i.e., K_b 7.4, is maintained close to 1 for Neu5Ac, while it is <1 for others (Table 1), suggesting a higher binding efficiency of PBA for SA in the intratumoral environment. Moreover, the presence of a methyl group at the C2 hydroxyl

15503

dx.doi.org/10.1021/ja406406h | *J. Am. Chem. Soc.* 2013, 135, 15501−15507

group of Me-SA reduced the binding constant, K_b, from 12.3 M^{-1} for SA to 3.4 M^{-1} for MeSA at pH 7.4 (Table 1). At pH 6.5, even though K_b decreased from 12.7 M^{-1} for SA to 6 M^{-1} for Me-SA, this binding constant was higher than the binding constants for the other sugars, indicating the selectivity of PBA for biological relevant SA at intratumoral pH (Table 1). Moreover, as K_b for Me-SA is higher at intratumoral pH than at physiological pH, it is expected that while the complex between PBA and SA will compete with other sugars in the bloodstream (pH 7.4), the PBA-installed micelles would primarily target SA under increasingly acidic conditions relevant to the environment of tumors.

Preparation and Characterization of PBA-Installed DACHPt-Loaded Micelles. Micelles were self-assembled due to the metal−polymer complexation between the carboxylic group of the PLGA and the platinum of DACHPt (Figure 1). Dynamic light scattering (DLS) measurements showed that the diameters of DACHPt/m and PBA-DACHPt/m were comparable, i.e., ~30 nm by weight distribution (Figure 3 and Table
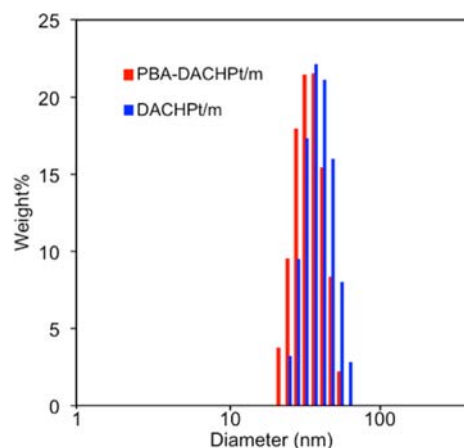
Figure 3. Diameter of DACHPt/m and PBA-DACHPt/m by weight distribution determined by DLS.

Table 2. Diameter, Polydispersity, Drug Loading and ζ Potential of DACHPt/m and PBA-DACHPt/m

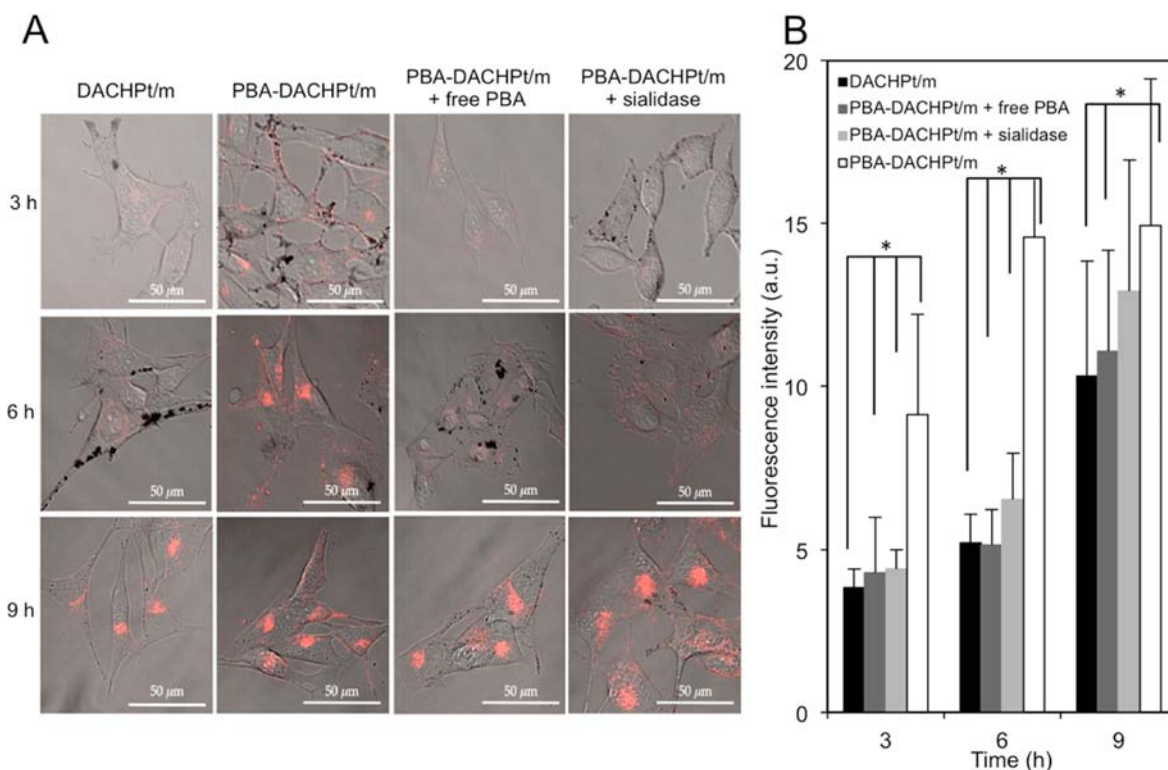|	DACHPt/m	PBA-DACHPt/m
diameter[a] (nm)	35	29
polydispersity index[a]	0.1	0.1
ζ potential (mV)[b]	−2.3 ± 1.4	−5.7 ± 0.3
Pt/polymer (wt/wt %)[c]	30	31
[Pt]/[COO] (mol/mol %)[c]	50	52

[a]Determined by weight% distribution obtained with DLS. [b]Determined in 10 mM phosphate buffer, pH 7.4. [c]Determined by ICP-MS.

2). Accordingly, these diameters may be suitable for achieving deep penetration in solid tumors, as we have recently demonstrated that 30 nm DACHPt/m can deeply penetrate even in poorly permeable malignancies.[35] Both micelles also showed comparable ζ potential values, which were slightly negative at pH 7.4 (Table 2). The Pt content in both micelles was found to be similar and remarkably high (Table 2), as determined by inductively coupled plasma mass spectrometry (ICP-MS). Moreover, in media containing chloride ions, i.e., 10 mM PBS plus 150 mM NaCl, DACHPt is released from the

core of the micelles by exchange reaction between chloride ions and carboxylic groups of PLGA.[32−34] Accordingly, the conjugation of PBA ligands did not affect the drug release rate of the micelles, and both DACHPt/m and PBA-DACHPt/m released ~40% of DACHPt after 2 days (Figure S3), which is similar to our previous reports.[32−34]

***In vitro* Targeting Ability of PBA-Installed DACHPt-Loaded Micelles.** The ability of PBA-DACHPt/m to bind SA epitopes in cancer cells was studied *in vitro*. First, we evaluated the cellular uptake of fluorescent-labeled micelles in B16F10 murine melanoma cells, which overexpress SA on the membrane,[23,36] by confocal laser microscopy. For constructing the fluorescent-labeled micelles, we conjugated Alexa Fluor 555 succinimidyl ester to the ω-amino group of MeO-PEG-*b*-PLGA and PBA-PEG-*b*-PLGA and obtained MeO-PEG-*b*-PLGA-Alexa$_{555}$ and PBA-PEG-*b*-PLGA-Alexa$_{555}$. The conjugation degree of Alexa Fluor 555 was 4 mol % for both polymers. We built the fluorescent micelles following the same method as for unlabeled micelles. After micelle formation, the fluorescence signal from the Alexa Fluor 555 probes in the core of the micelles was still detectable. Thus, after incubating the cells with the fluorescent micelles for 3 h, the fluorescent signal of PBA-DACHPt/m was significantly higher than that of DACHPt/m, indicating a faster cellular uptake (Figure 4A,B). After 6 h incubation, the difference between the micelles became more evident, as the fluorescent signal from PBA-DACHPt/m was localized inside the cells, while the signal from DACHPt/m was barely detectable (Figure 4A,B). After 9 h incubation, even though the fluorescent DACHPt/m was detected inside the tumor cells due to nonspecific uptake (Figure 4A,B), the fluorescent signal of PBA-DACHPt/m was still significantly higher (Figure 4B; $p < 0.001$). The addition of free PBA to the cell culture media reduced the cellular uptake of PBA-DACHPt/m, which showed a similar intensity to DACHPt/m (Figure 4A,B), indicating that the enhanced cellular uptake of PBA-DACHPt/m is due to the interaction of PBA moieties with the cells. Furthermore, treating the cells with sialidase, which is an enzyme that can cleave SA epitopes from the cells, before incubation with the micelles, led to a drastic decrease of the cellular internalization of PBA-DACHPt/m (Figure 4A,B), demonstrating the specific interaction of these micelles with SA epitopes on the cell membrane. For both free PBA- and sialidase-treated cells, the intracellular signal of fluorescent-labeled PBA-DACHPt micelles increased after 9 h incubation, comparable to nontargeted DACHPt/m with fluorescent-labeling, probably due to nonspecific uptake.

The enhancement of the antitumor effect of PBA-installed micelles was determined by evaluating the 50% growth inhibitory concentration (IC$_{50}$) against B16F10 cells. Moreover, the activity of the micelles was compared with that of oxaliplatin, because it is the clinically approved DACHPt-derivative and presents the same active complexes as the micelles. After exposing the cells to oxaliplatin or micelles for 3 h, the cells were washed and postincubated for 48 h. Thus, while free oxaliplatin showed lower IC$_{50}$ than both micelles, probably due to its rapid cellular internalization as well as the slow sustained release of DACHPt complexes from the micelles, the cytotoxicity of PBA-DACHPt/m was higher than that of DACHPt/m (Table 3), which correlated with the increased cellular uptake of these micelles, suggesting their potential for enhancing the therapeutic effect *in vivo*.

Figure 4. (A) Fluorescent microscopies of B16F10 cells incubated with fluorescent-labeled DACHPt/m or PBA- DACHPt/m for 3, 6, and 9 h. Free PBA was added 10 min before the addition of PBA- DACHPt/m for the competition assay. To cleave specifically SA, the cells were pretreated with sialidase before the incubation with PBA-DACHPt/m. The polymers were labeled with a fluorescent dye (Alexa Fluor 555; red). (B) Quantification of the fluorescence intensity. Data are expressed as averages ± S.E.M., $n = 20$, $*p < 0.001$.

Table 3. *In vitro* Cytotoxicity of Free Oxaliplatin, DACHPt/ m, and PBA-DACHPt/m after 48 h of Total Incubation Against B16F10 Cell Line

cells	IC$_{50}$ (μM)^a		
	oxaliplatin	DACHPt/m	PBA-DACHPt/m
B16F10	142 ± 5	278 ± 11	184 ± 8

^{a}Determined by WST-8 assay ($n = 8$).

***In vivo* Targeting Ability of PBA-Installed DACHPt-Loaded Micelles.** The performance of the micelles was evaluated *in vivo* in mice bearing B16F10 melanoma tumors. Accordingly, intravenously injected DACHPt/m and PBA-DACHPt/m showed similar prolonged blood circulation with ∼20% of injected dose per ml of plasma after 24 h (Figure 5A), which is in agreement with our previous results for DACHPt/ m,[32,34,35] suggesting the reduced interaction of PBA-DACHPt/ m with red blood cells and endothelial cells in the vasculature. This reduced interaction may be due to the interference by glucose in plasma, as normal glucose levels are ∼5 mM, while the concentration of SA in erythrocytes (SA$_{RBC}$) is ∼0.2 μM (20 nmol/10^9 cells).[48] Conversely, inside tumors, the glucose concentration decreases due to diffusion and the persistent metabolism of glucose to lactate in cancer cells.[49] Moreover, the metabolic products of this anaerobic glycolysis cause acidification of the intratumoral space, which decreases the binding constant for glucose (Table 1). Because the binding constant for SA at intratumoral pH is maintained and the SA amount on B16F10 cells is 1.1 nmol/10^6 cells,[23] which is more than 1000-fold higher than for erythrocytes, we expect that PBA-DACHPt/m effectively bind to tumor cells *in vivo*.

The tumor accumulation of DACHPt/m and PBA-DACHPt/m was similar up to 24 h, reaching ∼5% of the injected dose per g of tissue. However, 48 h after injection, the amount of DACHPt/m in the tumors declined, whereas PBA-DACHPt/m maintained their accumulation level in the tumor (Figure 5B; $p < 0.05$), suggesting that the interaction of PBA-DACHPt/m with the SA moieties on the surface of cancer cells improved the retention of micelles at the tumor site. As this prolonged tumor retention increases the exposure of the cancer cells to anticancer drugs, it may enhance the antitumor activity of PBA-DACHPt/m.

The antitumor activity of PBA-DACHPt/m was evaluated in an orthotopic tumor model prepared by intradermal inoculation of B16F10 cells to mice ($n = 5$). Mice were treated with intravenous injection three times at 2 day intervals, i.e., at days 0, 2, and 4, with oxaliplatin at dose of 8 mg/kg, and DACHPt/ m or PBA-DACHPt/m at a dose of 3 mg/kg. These doses were selected based on our previous observations for the maximum tolerated dose for oxaliplatin and the effective dose for DACHPt/m.[33] Thus, while free oxaliplatin failed to show any antitumor effect, probably due to its low accumulation in tumor tissues as well as its inactivation due to binding to serum proteins and erythrocytes after systemic administration,[50] both DACHPt/m and PBA-DACHPt/m significantly reduced the growth rate of the tumors, correlating with their enhanced accumulation in tumors (Figure 5B),with PBA-DACHPt/m showing higher efficacy than DACHPt/m ($p = 0.005$) (Figure 5C). Moreover, polymeric micelles can protect the Pt drug in their core during circulation and enhance the drug delivery to the nucleus of cancer cells,[34] therefore, increasing the *in vivo* antitumor efficacy of the Pt drug. In addition, this activity
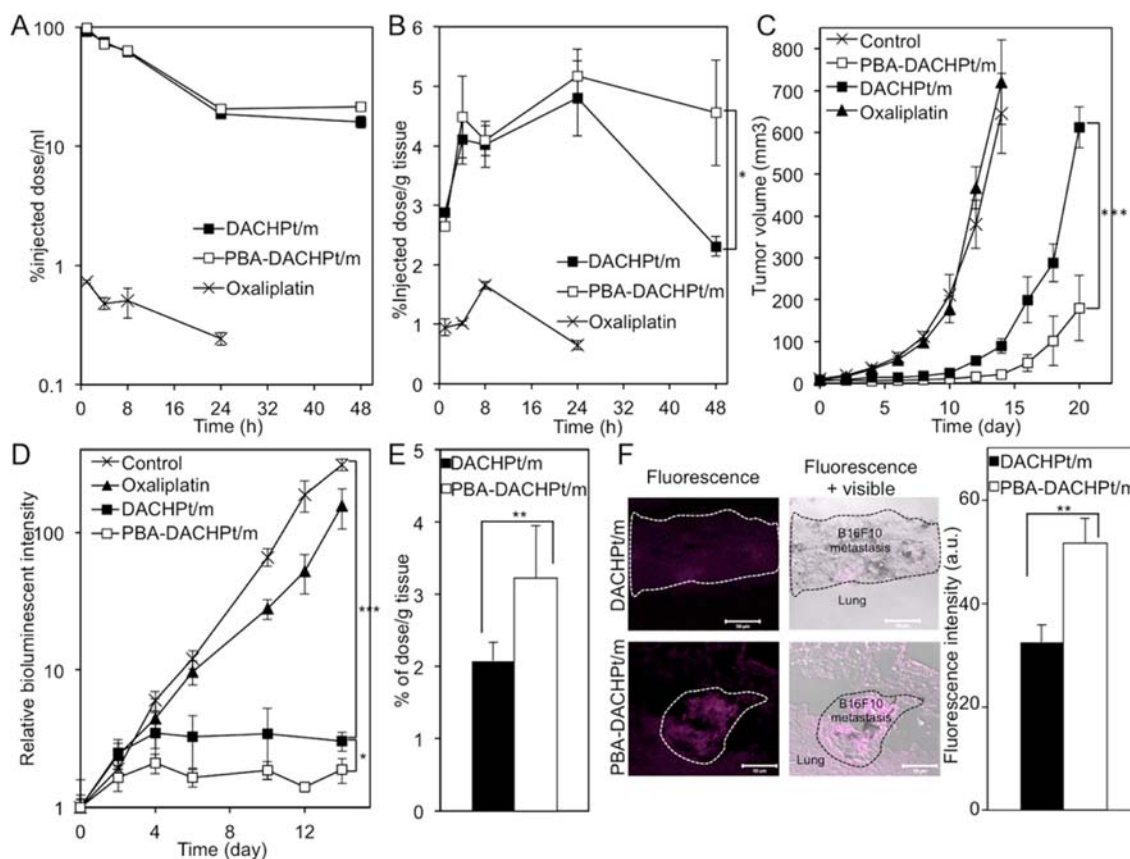
Figure 5. *In vivo* properties of PBA-DACHPt/m. (A) Plasma clearance and (B) tumor accumulation of DACHPt/m and PBA-DACHPt/m in mice bearing B16F10 tumor model. Data are means ± S.E.M.; $n = 5$; *$p < 0.05$. (C) Antitumor activity against orthotopic B16F10 tumors after treatment with oxaliplatin (8 mg/kg), DACHPt/m or PBA-DACHPt/m (3 mg/kg) injected on days 0, 2, and 4. Data are expressed as averages ± S.E.M.; $n = 5$; ***$p < 0.001$. (D) Antitumor activity against lung metastasis induced by B16F10-Luc melanoma cells. Data are expressed as averages ± S.E.M.; $n = 5$; *$p < 0.05$; ***$p < 0.001$. (E) Accumulation of micelles in lungs having B16F10-Luc melanoma cells 24 h after the intravenous injection. Data are expressed as averages ± S.E.M., $n = 6$, **$p < 0.005$. (F) Ex vivo fluorescent microscopies of lung tissues bearing B16F10-Luc metastasis 24 h after the injection of fluorescent-labeled DACHPt/m or PBA-DACHPt/m (Alexa Fluor 647; pink) and quantification of fluorescent intensity in metastatic regions. Data are expressed as averages ± S.E.M., $n = 3$, **$p < 0.005$.

enhancement did not come at the expense of side effects, and the body weight of the mice remained stable even after the repeated administration of the micelles (Figure S4).

In addition, as metastasis is the major cause of cancer-related death and because the expression of SA is highly associated with the metastatic disease,[18] we evaluated the efficiency of PBA-DACHPt/m against bioluminescent lung metastasis, obtained after intravenous injection of B16F10 cells expressing luciferase (B16F10-Luc) in BALB/c nu/nu mice. Mice were treated intravenously three times at 2 day intervals, i.e., at days 0, 2, and 4, with oxaliplatin at dose of 8 mg/kg, DACHPt/m or PBA-DACHPt/m at a dose of 3 mg/kg. By following the growth of metastasis through imaging the bioluminescence signal, we observed that, while oxaliplatin showed no antitumor effect (Figure 5D), both DACHPt/m and PBA-DACHPt/m significantly inhibited the progression of the metastasis. Again, PBA-DACHPt/m demonstrated to be more efficacious than DACHPt/m, showing 2-fold lower bioluminescent intensity (Figure 5D; $p < 0.05$). The enhanced activity of PBA-DACHPt/m matched the increased Pt accumulation of these micelles in metastatic lungs 24 h after injection (Figure 5E). Moreover, the specificity of PBA-DACHPt/m to the metastatic sites in lungs was confirmed by histology after the injection of micelles labeled with Alexa Fluor 647 (Figure 5F). Thus, the fluorescence intensity for PBA-DACHPt/m was higher than

that for DACHPt/m at the metastatic regions, supporting the superior efficacy of PBA-DACHPt/m.

■ CONCLUSION

Our findings demonstrated that PBA conjugation of the surface of polymeric micellar nanocarriers enhanced their tumor targeting ability, by specific interaction with SA epitopes overexpressed in tumor cells, without affecting their long circulating properties. These results support the application of borate ester chemistry for specific targeting of tumor-associated carbohydrate antigens at intratumoral pH conditions. Moreover, because of the clear relationship between overexpression of sialylated epitopes, tumor aggressiveness, and patients' prognosis as well as the safety and nonimmunogenicity of the approach, PBA-mediated targeting of nanocarriers offers a highly translational approach for clinical diagnosis and therapy of solid tumors.

■ ASSOCIATED CONTENT

S **Supporting Information**

Experimental section, preparation scheme, and ^{1}H NMR of PBA-PEG-*b*-PLGA, study of the pK_a of PBA-PEG-*b*-PLGA, the release rate profiles of the micelles and their in vivo toxicity are provided. This material is available free of charge via the Internet at http://pubs.acs.org.

■ AUTHOR INFORMATION

Corresponding Author

kataoka@bmw.t.u-tokyo.ac.jp

Author Contributions

◆These authors contributed equally.

Notes

The authors declare no competing financial interest.

■ REFERENCES

(1) Davis, M. E.; Chen, Z.; Shin, D. M. *Nat. Rev. Drug Discovery* **2008**, *7*, 771.

(2) Peer, D.; Karp, J. M.; Hong, S.; Farokhzad, O. C.; Margalit, R.; Langer, R. *Nat. Nanotechnol.* **2007**, *2*, 751.

(3) Duncan, R. *Curr. Opin. Biotechnol.* **2011**, *22*, 492.

(4) Nishiyama, N.; Kataoka, K. *Pharmacol. Ther.* **2006**, *112*, 630.

(5) Miyata, K.; Christie, R. J.; Kataoka, K. *React. Funct. Polym.* **2011**, *7*, 227.

(6) Matsumura, Y.; Maeda, H. *Cancer Res.* **1986**, *46*, 6387.

(7) Allen, T. M. *Nat. Rev. Cancer* **2002**, *2*, 750.

(8) Torchilin, V. *Expert Opin. Drug Deliv.* **2008**, *5*, 1003.

(9) Cheng, W. W.; Allen, T. M. *Expert Opin Drug Delivery* **2010**, *7*, 461.

(10) Farokhzad, O. C.; Cheng, J.; Teply, B. A.; Sherifi, I.; Jon, S.; Kantoff, P. W.; Richie, J. P.; Langer, R. *Proc. Natl. Acad. Sci. U.S.A.* **2006**, *103*, 6315.

(11) Zhang, X.-X.; Eden, H. S.; Chen, X. *J. Controlled Release* **2012**, *159*, 2.

(12) Oba, M.; Vachutinsky, Y.; Miyata, K.; Kano, M. R.; Ikeda, S.; Nishiyama, N.; Itaka, K.; Miyazono, K.; Koyama, H.; Kataoka, K. *Mol. Pharmaceutics* **2010**, *7*, 501.

(13) Bae, Y.; Jang, W. D.; Nishiyama, N.; Fukushima, S.; Kataoka, K. *Mol. Biosyst.* **2005**, *1*, 242.

(14) Hakomori, S. *Cancer Res.* **1996**, *56*, 5309.

(15) Dube, D. H.; Bertozzi, C. R. *Nat. Rev. Drug Discovery* **2006**, *4*, 477.

(16) Xu, Y.; Sette, A.; Sidney, J.; Gendler, S. J.; Franco, A. *Immunol. Cell Biol.* **2005**, *83*, 440.

(17) Kannagi, R.; Sakuma, K.; Miyazaki, K.; Lim, K. T.; Yusa, A.; Yin, J.; Izawa, M. *Cancer Sci.* **2010**, *101*, 586.

(18) Kannagi, R.; Izawa, M.; Koike, T.; Miyazaki, K.; Kimura, N. *Cancer Sci.* **2004**, *95*, 377.

(19) Sharon, N. *J. Biol. Chem.* **2007**, *282*, 2753.

(20) Koprowski, H.; Herlyn, M.; Steplewski, Z.; Sears, H. F. *Science* **1981**, *212*, 53.

(21) Durocher, J. R.; Payne, R. C.; Conrad, M. E. *Blood* **1975**, *45*, 11.

(22) Born, G. V.; Palinski, W. *Br. J. Exp. Pathol.* **1985**, *66*, 543.

(23) Matsumoto, A.; Cabral, H.; Sato, N.; Kataoka, K.; Miyahara, Y. *Angew. Chem., Int. Ed.* **2010**, *49*, 5494.

(24) Otsuka, H.; Uchimura, E.; Koshino, H.; Okano, T.; Kataoka, K. *J. Am. Chem. Soc.* **2003**, *125*, 3493.

(25) Djanashvili, K.; Frullano, L.; Peters, J. A. *Chem.—Eur. J.* **2005**, *11*, 4010.

(26) Geninatti Crich, S.; Alberti, D.; Szabo, I.; Aime, S.; Djanashvili, K. *Angew. Chem., Int. Ed.* **2013**, *52*, 1161.

(27) Kataoka, K.; Harada, A.; Nagasaki, Y. *Adv. Drug Delivery Rev.* **2001**, *47*, 113.

(28) Osada, K.; Christie, R. J.; Kataoka, K. *J. R. Soc. Interface* **2009**, *6*, S325.

(29) Cabral, H.; Kataoka, K. *Sci. Technol. Adv. Mater.* **2010**, *11*, 014109.

(30) Matsumura, Y.; Kataoka, K. *Cancer Sci.* **2009**, *100*, 572.

(31) Plummer, R.; Wilson, R. H.; Calvert, H.; Boddy, A. V.; Griffin, M.; Sludden, J.; Tilby, M. J.; Eatock, M.; Pearson, D. G.; Ottley, C. J.; Matsumura, Y.; Kataoka, K.; Nishiya, T. *Br. J. Cancer* **2011**, *104*, 593.

(32) Cabral, H.; Nishiyama, N.; Okazaki, S.; Koyama, H.; Kataoka, K. *J. Controlled Release* **2005**, *101*, 223.

(33) Cabral, H.; Nishiyama, N.; Kataoka, K. *J. Controlled Release* **2007**, *121*, 146.

(34) Murakami, M.; Cabral, H.; Matsumoto, Y.; Wu, S.; Kano, M. R.; Yamori, T.; Nishiyama, N.; Kataoka, K. *Sci. Transl. Med.* **2011**, *3*, 64ra2.

(35) Cabral, H.; Matsumoto, Y.; Mizuno, K.; Chen, Q.; Murakami, M.; Kimura, M.; Terada, Y.; Kano, M. R.; Miyazono, K.; Uesaka, M.; Nishiyama, N.; Kataoka, K. *Nat. Nanotechnol.* **2011**, *6*, 815.

(36) Kinoshita, Y.; Sato, S.; Takeuchi, T. *Cell. Struct. Funct.* **1989**, *14*, 35.

(37) Springsteen, G.; Wang, B. *Tetrahedron* **2002**, *58*, 5291.

(38) Levonis, S. M.; Kiefel, M. J.; Houston, T. A. *Chem. Commun.* **2009**, *17*, 2278.

(39) Teichert, J. F.; Mazunin, D.; Bode, J. W. *J. Am. Chem. Soc.* **2013**, *135*, 11314.

(40) Regueiro-Figueroa, M.; Djanashvili, K.; Esteban-Gómez, D.; de Blas, A.; Platas-Iglesias, C.; Rodríguez-Blas, T. *Eur. J. Org. Chem.* **2010**, 3237.

(41) DiCesare, N.; Lakowicz, J. R. *J. Phys. Chem. A* **2001**, *105*, 6834.

(42) Sun, X.-Y.; Liu, B.; Jiang, Y.-B. *Anal. Chim. Acta* **2004**, *515*, 285.

(43) Martin, G. R.; Jain, R. K. *Cancer Res.* **1994**, *54*, 5670.

(44) James, T. D.; Sandanayake, K. R. A. S.; Shinkai, S. *Nature* **1995**, *374*, 345.

(45) James, T. D.; Sandanayake, K. R. A. S.; Shinkai, S. *Angew. Chem., Int. Ed.* **1996**, *35*, 1919.

(46) Mori, Y.; Suzuki, A.; Yoshino, K.; Kakihana, H. *Pigm. Cell Res.* **1989**, *2*, 273.

(47) Tomsho, J. W.; Benkovic, S. J. *J. Org. Chem.* **2012**, *77*, 2098.

(48) Miller, A.; Sullivan, J. F.; Katz, J. H. *Cancer Res.* **1963**, *23*, 485.

(49) Gatenby, R. A.; Gillies, R. J. *Nat. Rev. Cancer* **2004**, *4*, 891.

(50) Graham, M. A.; Lockwood, G. F.; Greenslade, D.; Brienza, S.; Bayssas, M.; Game, E. *Clin. Cancer Res.* **2000**, *6*, 1205.